An asteroseismic study of the β Cephei star θ Ophiuchi: constraints on global stellar parameters and core overshooting

M. Briquet,[1*][†] T. Morel,[1][‡] A. Thoul,[2][§] R. Scuflaire,[2] A. Miglio,[2] J. Montalbán,[2] M.-A. Dupret[3] and C. Aerts[1,4]

[1]*Instituut voor Sterrenkunde, Katholieke Universiteit Leuven, Celestijnenlaan 200 D, B-3001 Leuven, Belgium*
[2]*Institut d'Astrophysique et de Géophysique de Liège, Université de Liège, allée du Six Août 17, B-4000 Liège, Belgium*
[3]*Observatoire de Paris, LESIA, 5 place Jules Janssen, 92195 Meudon Principal Cedex, France*
[4]*Department of Astrophysics, University of Nijmegen, PO Box 9010, 6500 GL Nijmegen, the Netherlands*

ABSTRACT

We present a seismic study of the β Cephei star θ Ophiuchi. Our analysis is based on the observation of one radial mode, one rotationally split $\ell = 1$ triplet and three components of a rotationally split $\ell = 2$ quintuplet for which the m values were well identified by spectroscopy. We identify the radial mode as fundamental, the triplet as p_1 and the quintuplet as g_1. Our non-local thermodynamic equilibrium abundance analysis results in a metallicity and CNO abundances in full agreement with the most recent updated solar values. With $X \in [0.71, 0.7211]$ and $Z \in [0.009, 0.015]$, and using the Asplund et al. mixture but with a Ne abundance about 0.3 dex larger, the matching of the three independent modes enables us to deduce constrained ranges for the mass ($M = 8.2 \pm 0.3\,\mathrm{M}_{\odot}$) and central hydrogen abundance ($X_c = 0.38 \pm 0.02$) of θ Oph and to prove the occurrence of core overshooting ($\alpha_{\mathrm{ov}} = 0.44 \pm 0.07$). We also derive an equatorial rotation velocity of $29 \pm 7\,\mathrm{km\,s^{-1}}$. Moreover, we show that the observed non-equidistance of the $\ell = 1$ triplet can be reproduced by the second-order effects of rotation. Finally, we show that the observed rotational splitting of two modes cannot rule out a rigid rotation model.

Key words: stars: abundances – stars: early-type – stars: individual: θ Oph – stars: interiors – stars: oscillations.

1 INTRODUCTION

From the last few years, many breakthroughs have been achieved in the field of asteroseismology of β Cephei stars, thanks to several observational photometric and spectroscopic multisite campaigns and long-term monitoring dedicated to this kind of pulsating B-type stars. The aim is to improve our knowledge of their internal structure and more precisely of two mixing processes that affect their evolutionary path: core overshooting and internal rotation.

The first detailed asteroseismic modelling was performed for V836 Cen, which led to constraints not only on global stellar parameters but also on the core overshooting parameter. Moreover, the non-rigid rotation of the star was proved (Aerts et al. 2003; Dupret et al. 2004). Similar results were afterwards obtained for ν Eri (Ausseloos et al. 2004; Pamyatnykh, Handler & Dziembowski 2004). Recently, Aerts, Marchenko & Matthews (2006) gave con-

straints on the physical parameters of δ Ceti, thanks to the discovery of low-amplitude modes by the satellite MOST. Finally, the seismic interpretation by Mazumdar et al. (2006) showed the occurrence of core overshooting for β CMa. The derived overshooting parameter values are 0.10 ± 0.05, 0.05 ± 0.05, 0.20 ± 0.05 and 0.20 ± 0.05 for V836 Cen, ν Eri, δ Ceti and β CMa, respectively.

The β Cephei star θ Ophiuchi was also the subject of intensive photometric and spectroscopic observations as described in Handler, Shobbrook & Mokgwetsi (2005) and Briquet et al. (2005) (hereafter Paper I and Paper II), respectively. It was found that θ Oph has a frequency spectrum which is similar to that of V836 Cen. In this paper, we present our modelling based on accurate frequency determination and successful mode identification obtained in Papers I and II. Our main objective is to test if the occurrence of core overshooting and non-rigid rotation found for V836 Cen also applies to θ Oph.

The paper is organized as follows. In Section 2, we summarize the observational pulsation constraints which constitute the starting point of our seismic modelling of θ Oph. In Section 3, we perform a detailed abundance analysis of θ Oph with the aim to use the deduced metallicity as an additional constraint. In Section 4, we present the evolution and the oscillation codes that we used in our study, as well

*E-mail: maryline@ster.kuleuven.be
†Postdoctral Fellow of the Fund for Scientific Research, Flanders
‡European Space Agency (ESA) postdoctoral external fellow
§Chercheur qualifié FNRS

Table 1. The pulsation modes derived from the photometric and the spectroscopic results presented in Papers I and II, respectively. The amplitudes of the modes are given for the u filter and for the radial velocities.

ID	Frequency (d^{-1})	(ℓ, m)	u amplitude (mmag)	RV amplitude (km s^{-1})
ν_1	7.1160	$(2, -1)$	12.7	2.54
ν_2	7.2881	$(2, 1)$	2.1	–
ν_3	7.3697	$(2, 2)$	3.6	–
ν_4	7.4677	$(0, 0)$	4.7	2.08
ν_5	7.7659	$(1, -1)$	3.4	–
ν_6	7.8742	$(1, 0)$	2.3	–
ν_7	7.9734	$(1, 1)$	2.4	–

Figure 1. The error boxes represent the position of θ Oph in the HR diagram as derived from photometric (full line, Paper I) and spectroscopic data (dashed line, Paper II; dotted line, this paper). The positions of the models which fit exactly the three independent modes are also shown for the different couples $(Z, \alpha_{\rm ov})$ given in Table 4.

as the physical inputs. In Section 5, we derive the seismic constraints on global stellar parameters and on core overshooting. In Section 6, we test the hypothesis of a non-rigid rotation model thanks to the two observed multiplets. We end with a conclusion in Section 7.

2 OBSERVATIONAL CONSTRAINTS

The observational pulsation characteristics of θ Oph derived in Papers I and II can be summarized as follows. The photometric data (Paper I) were gathered in the framework of a three-site campaign, allowing the detection of seven pulsation frequencies. The identification of their corresponding ℓ value showed the presence of one radial mode, one rotationally split $\ell = 1$ triplet and three components of a rotationally split $\ell = 2$ quintuplet. In addition, the spectroscopic observations (Paper II) lifted the ambiguity for the m value of the observed $\ell = 2$ main mode. The pulsation frequencies and their (ℓ, m) values are listed in Table 1. We note that such a frequency spectrum was observed for the star V836 Cen (Aerts et al. 2004). We also point out that the mode identifications of all the observed components of the quintuplet are determined for θ Oph, which was not the case for V836 Cen.

The position of appropriate models will be compared with the position of the star in the HR diagram that was determined photometrically and spectroscopically in Papers I and II. The obtained error boxes are represented in Fig. 1. We note that such a deviation between photometrically and spectroscopically derived effective temperatures is common for B-type stars (e.g. De Ridder et al. 2004; Morel et al. 2006).

Recently, Niemczura & Daszynska-Daszkiewicz (2005) determined [M/H] for θ Oph. However, they did not have information that θ Oph is a triple system composed of a B2 primary, a spectroscopic secondary with a mass lower than 1 M$_\odot$ (Briquet et al. 2005) and a speckle B5 star (McAlister et al. 1993). In what follows, we present a careful abundance analysis for the primary by taking into account the presence of the tertiary, the contribution to the lines of the secondary being negligible.

3 ABUNDANCE ANALYSIS

The non-local thermodynamic equilibrium (NLTE) abundances of He, C, N, O, Mg, Al, Si, S and Fe were calculated using the latest versions of the line formation codes DETAIL/SURFACE and plane-parallel, fully line-blanketed Kurucz atmospheric models (Kurucz 1993). Curve-of-growth techniques were used to determine the abundances using the equivalent widths of a set of unblended lines measured in a mean CORALIE spectrum (see Paper II), which was created by co-adding the 86 individual exposures (all put in the laboratory rest
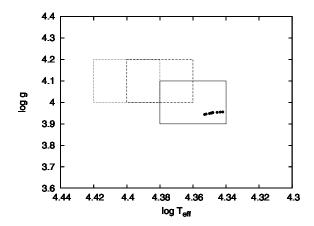
frame prior to this operation). The reader is referred to Morel et al. (2006) for complete details on the methodology used to derive the elemental abundances.

To correct for the contamination of the spectrum by the tertiary, our study is based on synthetic, composite spectra assuming the following parameters for this companion: $T_{\rm eff} = 19\,000$ K, $\log g = 4.0$ dex [cgs] (Paper II) and a microturbulent velocity, $\xi = 5$ km s^{-1}, typical of B-type dwarfs. We also considered that the tertiary contributes to 22 per cent of the total light of the system in the optical band (Paper I). In addition, we assumed the star to have a chemical composition typical of OB dwarfs in the solar vicinity (Daflon & Cunha 2004). For iron, we assumed an abundance $\log \epsilon({\rm Fe}) = 7.3$ dex (Morel et al. 2006). We will examine below the sensitivity of our results to these assumptions.

A standard, iterative scheme is first used to self-consistently derive the atmospheric parameters: $T_{\rm eff}$ is determined from the Si II/III ionization balance, $\log g$ from fitting the collisionally broadened wings of the Balmer lines and ξ from requiring the abundances yielded by the O II features to be independent of the line strength. We obtain: $T_{\rm eff} = 25\,000 \pm 1000$ K, $\log g = 4.10 \pm 0.15$ dex [cgs] and $\xi = 4^{+2}_{-3}$ km s^{-1}. For comparison, we obtained in Paper II, $T_{\rm eff} = 24\,000 \pm 1000$ K and $\log g = 4.1 \pm 0.1$ dex [cgs] using the NLTE code FASTWIND (Puls et al. 2005). Other studies show that using different methods on the same data set can indeed lead to uncertainties of the order of 500 K for B-type stars (e.g. Smalley & Dworetsky 1995; Kaiser 2006; Morel et al. 2006).

The abundances are given in Table 2 and compared with the standard solar mixture of Grevesse & Sauval (1998) and with values derived from time-dependent, three-dimensional hydrodynamical models (Asplund et al. 2005, and references therein). The quoted uncertainties take into account both the line-to-line scatter and the errors arising from the uncertainties on the atmospheric parameters. Note that a possible downward revision of $T_{\rm eff}$ by $\sim$1000 K (see above) is explicitly taken into account in the total error budget. We infer a low helium content, but this quantity is uncertain and may be considered solar within the large error bars. On the other hand, there is no indication for the nitrogen excess occasionally observed in other slowly rotating β Cephei stars (Morel et al. 2006). The resulting metallicity, $Z = 0.0114 \pm 0.0028$, is identical, within the errors, to the most recent and likely realistic estimates

Table 2. Mean NLTE abundances (on the scale in which $\log \epsilon[\mathrm{H}] = 12$) and total 1σ uncertainties. The number of used spectral lines is given in brackets. For comparison purposes, we provide in the last two columns the standard solar composition of Grevesse & Sauval (1998; Sun 1D) and updated values in the present-day solar photosphere derived from 3D hydrodynamical models (Asplund et al. 2005; Sun 3D).

	θ Oph	Sun 1D	Sun 3D
He/H	0.066 ± 0.026 (10)	0.085 ± 0.001	0.085 ± 0.002
$\log \epsilon$(C)	8.32 ± 0.09 (7)	8.52 ± 0.06	8.39 ± 0.05
$\log \epsilon$(N)	7.78 ± 0.10 (23)	7.92 ± 0.06	7.78 ± 0.06
$\log \epsilon$(O)	8.58 ± 0.26 (27)	8.83 ± 0.06	8.66 ± 0.05
$\log \epsilon$(Mg)	7.49 ± 0.15 (2)	7.58 ± 0.05	7.53 ± 0.09
$\log \epsilon$(Al)	6.24 ± 0.14 (4)	6.47 ± 0.07	6.37 ± 0.06
$\log \epsilon$(Si)	7.04 ± 0.22 (8)	7.55 ± 0.05	7.51 ± 0.04
$\log \epsilon$(S)	7.22 ± 0.27 (5)	7.33 ± 0.11	7.14 ± 0.05
$\log \epsilon$(Fe)	7.41 ± 0.17 (27)	7.50 ± 0.05	7.45 ± 0.05
Z	0.0114 ± 0.0028	0.0172 ± 0.0012	0.0124 ± 0.0007

for the Sun (Table 2). To calculate this quantity, the abundances of the elements not under the study were taken from Grevesse & Sauval (1998). Our assumed neon abundance is indistinguishable from recent values derived for a sample of B-type stars in the Orion association (Cunha, Hubeny & Lanz 2006). The other species are trace elements and contribute only negligibly to metal mass fraction.

To examine the sensitivity of our results to the various assumptions made about the physical properties of the companion, we have repeated the abundance analysis after varying the adopted effective temperature, surface gravity, chemical composition and luminosity of the tertiary within the range of plausible values. Namely, we assumed in turn: $T_{\mathrm{eff}} = 21\,000$ K, $\log g = 3.7$ dex [cgs], the abundances of all the metals enhanced by 0.3 dex relative to solar and a contribution of only 18 per cent to the total light of the system in the optical, while keeping the other parameters unchanged. As expected, the abundances of the chemical elements determined from lines of low-ionization ionic species (e.g. Mg, S) are most strongly affected by the choice of the parameters for the cool component (Table 3). However, the metallicity remains largely unaltered in all the cases. Our conclusions regarding the metal content of θ Oph appear therefore robust against the exact nature of its speckle companion.

Table 3. Sensitivity of the derived metal abundances and metallicity of θ Oph on the assumed properties of the tertiary. We quote the abundance differences compared with the values listed in Table 2.

	$\Delta T_{\mathrm{eff}} =$ +2000 K	$\Delta \log g =$ −0.3 dex	$\Delta \log \epsilon =$ +0.3 dex	Flux ratio = 18 per cent
$\Delta \log \epsilon$(C)	−0.05	−0.02	−0.05	−0.01
$\Delta \log \epsilon$(N)	−0.05	−0.02	−0.03	−0.02
$\Delta \log \epsilon$(O)	−0.06	−0.02	−0.03	−0.03
$\Delta \log \epsilon$(Mg)	+0.06	+0.02	−0.15	+0.02
$\Delta \log \epsilon$(Al)	−0.05	−0.01	−0.04	−0.01
$\Delta \log \epsilon$(Si)	+0.05	+0.01	−0.15	+0.03
$\Delta \log \epsilon$(S)	+0.12	+0.00	−0.44	+0.05
$\Delta \log \epsilon$(Fe)	−0.04	−0.02	−0.04	−0.02
ΔZ	−0.0007	−0.0003	−0.0011	−0.0003

4 STELLAR MODELS

The numerical tools and physical inputs used in our study are the following. The stellar models for non-rotating stars were computed with the evolutionary code CLÉS (Code Liégeois d'Évolution Stellaire; Scuflaire et al. 2007a). We used the OPAL2001 equation of state (Rogers & Nayfonov 2002) and Caughlan & Fowler (1988) nuclear reaction rates with Formicola et al. (2004) for the $^{14}\mathrm{N}(p, \gamma)^{15}\mathrm{O}$ cross-section. Convective transport is treated by using the classical Mixing Length Theory of convection (Böhm-Vitense 1958). As shown in the previous section, the abundances of θ Oph are in full agreement with the solar values of Asplund et al. (2005). For the chemical composition, we consequently used the solar mixture from these authors, except for Ne. For this latter element, a direct abundance determination in a small sample of nearby B stars using photospheric lines (Cunha et al. 2006) suggests a value ∼0.3 dex larger than quoted by Asplund et al. (2005). For our computations, we consequently adopted $\log \epsilon(\mathrm{Ne}) = 8.11$. We used OP opacity tables (Seaton 2005) computed for the mixture in Cunha et al. (2006) [i.e. the mixture of Asplund et al. 2005 and $\log \epsilon(\mathrm{Ne}) = 8.11$]. These tables are completed at $\log T < 4.1$ with the low temperature tables of Ferguson et al. (2005) for the Asplund et al. (2005) mixture, as the effect of increasing Ne on low temperature opacities can be neglected for such a hot star. We computed stellar models with and without taking into account microscopic diffusion. For models with diffusion, we used the formulation of Thoul, Bahcall & Loeb (1994).

Stellar models are parametrized by the initial hydrogen abundance X, the core convective overshooting parameter α_{ov}, the metallicity Z, the mass M and the central hydrogen abundance X_{c} (which is related to the age).

For each stellar model, we calculated the theoretical frequency spectrum of low-order p and g modes with a degree of the oscillation up to $\ell = 2$ using a standard adiabatic code (Scuflaire et al. 2007b), which is much faster than a non-adiabatic code but leads to the same theoretical pulsation frequencies within the adopted precision of the fit, which was 10^{-3} d^{-1}. Once the models fitting the observed modes are selected, we checked the excitation of the pulsation modes with the linear non-adiabatic code MAD developed by Dupret (2001).

In an attempt to explain the asymmetries of the observed multiplets, we also computed the adiabatic frequencies with the code FILOU (Tran Minh & Léon 1995), which includes effects of rotation up to the second order, according to the formalism of Soufi, Goupil & Dziembowski (1998).

5 CONSTRAINTS ON STELLAR PARAMETERS AND CORE OVERSHOOTING

5.1 Effects of diffusion

θ Oph is a slow rotator with an equatorial rotation velocity of about 30 km s^{-1} (Paper II). Moreover, its surface convection zone is very thin. In such conditions, diffusion mechanisms can occur and alter the photospheric abundances. We consequently investigated if diffusion could be the explanation for the marginal lower He content of θ Oph compared to the solar value. Moreover, we checked its effect on the oscillation frequencies.

Our calculations include microscopic diffusion (without radiative forces and wind, and using TBL94's routine; Thoul et al. 1994) and a turbulent mixing consistent with the results of Talon et al. (1997). We were able to reproduce the observed surface metallicity and helium abundances with models having initially the solar composition ($X = 0.7211$, $Y = 0.264$ and $Z = 0.01\,485$). Those models
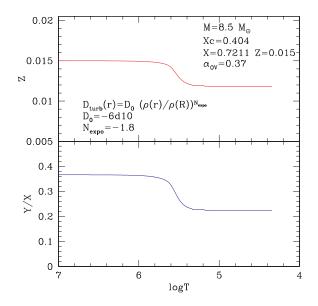
Figure 2. Metallicity and Y/X profiles for a model which fits the three observed frequencies and has both a solar initial composition and a surface composition compatible with the observations.

are very close to those obtained without diffusion, because the diffusion only affects the very superficial layers of the star. In particular, the models calculated with and without diffusion have exactly the same frequency spectrum. In Fig. 2, we show the metallicity and the Y/X profiles for a model which fits the three observed frequencies and has both a solar initial composition and a surface composition compatible with the observations. The diffusion and the turbulent mixing only affect layers down to a radius of $0.92R$.

Even though these results agree very well with the observations, it might be hazardous to trust them blindly. Indeed, radiative accelerations and stellar winds are very important in those stars and can strongly affect the surface abundances (Bourge et al. 2006). They were ignored here because calculations involving those effects are computationally intensive and difficult to perform, and clearly beyond the scope of this paper.

5.2 Seismic analysis

Since considering or not considering diffusion does not affect the derived stellar parameters of our models, we continued our analysis without diffusion but by considering sufficiently large ranges for X and Z.

For our seismic analysis, we first searched for models that fit the radial mode with frequency ν_4 together with the zonal $\ell = 1$ mode with frequency ν_6. We then made use of the quintuplet to add additional constraints.

We found that the radial mode is either the fundamental mode or the first overtone. However, the models with ν_4 as the first overtone are further away from the observational position in the HR diagram than the models with ν_4 as fundamental. Moreover, none of the three modes is excited by the classical κ mechanism for models with ν_4 as the first overtone, even for a value of Z of 0.015 with Y of 0.0264. We consequently concluded that the radial mode is identified as fundamental and a scan of stellar parameter space also reveals that the triplet is identified as p_1.

Fitting one frequency results in finding one model along the evolutionary track for every combination of X, α_{ov}, Z and M. Then, X being fixed, fitting two frequencies gives a relation between two
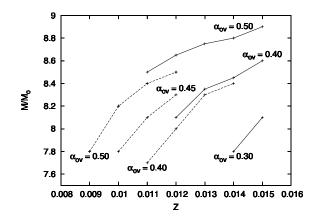

Figure 3. The M–Z relations obtained by matching the radial mode and the central peak of the triplet for several values of the core overshooting parameter, X being fixed to 0.71 (dashed lines) or 0.7211 (full lines).

Table 4. Relation between Z and α_{ov} imposed by the matching of the three independent modes.

Z	α_{ov}
0.009	0.51
0.010	0.48
0.011	0.45
0.012	0.43
0.013	0.40
0.014	0.38
0.015	0.37

parameters for given values of the last one. For the considered values of α_{ov}, one thus gets several M–Z relations that are shown in Fig. 3. We can see that the fitting of the two frequencies implies an increase in mass if either the metallicity or the core convective overshooting parameter increases. This figure also illustrates the order of magnitude difference in mass induced by different adopted X values.

Because the zonal mode of the quintuplet was not observed, we computed it as the average frequency of the two surrounding modes with frequency ν_1 and ν_2. A scan of stellar parameter space shows that the quintuplet is identified as g_1. The fitting of a third independent frequency implies a relation between the metallicity and the core overshooting parameter: the lower the metallicity the higher the overshooting. This α_{ov}–Z relation is presented in Table 4.

The positions in the HR diagram of the models reproducing the observed modes are shown in Fig. 1 for several couples (Z, α_{ov}). One can see that the derived models are situated in the cooler part of the photometric observed error box, and outside the spectroscopic one. This is actually the case for all studied β Cephei stars up to now and needs to be further investigated. By considering a wide range of metallicities $Z \in [0.009, 0.015]$, for $X \in [0.71, 0.7211]$, one obtains a core overshooting parameter $\alpha_{ov} \in [0.37, 0.51]$ and a mass $M \in [7.9, 8.5] \, M_\odot$. The other physical parameters are given in Table 5. The three modes are well excited by the classical κ mechanism for a metallicity larger than 0.011. However, radiatives' forces on iron allow this element to accumulate in the excitation region and lead to the excitation of additional modes in lower metallicity

Table 5. Physical parameters of the model that matches the observed modes, $X \in [0.71, 0.7211]$ and $Z \in [0.009, 0.015]$.

M (M$_\odot$)	=	8.2 ± 0.3
T_{eff} (K)	=	$22\,260 \pm 280$
$\log g$ (dex)	=	3.950 ± 0.006
X_{c}	=	0.38 ± 0.02
α_{ov}	=	0.44 ± 0.07

stars (Bourge et al. 2006; Pamyatnykh et al. 2004). Note that the only other theoretically excited mode with $\ell \leqslant 2$ is the f mode with $\ell = 1$ but only for Z larger than 0.013.

We point out that models matching the observed modes but computed using the solar abundances of Grevesse & Sauval (1998) with OPAL opacity tables are not excited for $Z \sim 0.01$. We refer to Miglio, Montalbán & Dupret (2007) for a detailed discussion on the implication of the adopted opacity tables and metal mixtures on the excitation of pulsation modes.

We also mention that the amount of overshooting found for θ Oph corresponds exactly to that computed by Deupree (2000) by means of 2D hydrodynamic simulations of zero-age main-sequence convective cores. Our derived value is also in agreement with results obtained by Ribas, Jordi & Gimenez (2000) who provided an empirical calibration of convective core overshooting for a range of stellar masses by studying eight detached double-lined eclipsing binaries. They found a systematic increase in the amount of convective overshooting with the stellar mass, the values being 0.3–0.6 for $\sim 10\,\text{M}_\odot$ stars.

6 CONSTRAINTS ON THE ROTATION

6.1 First-order analysis

When the rotation frequency is small compared to both $\sqrt{R^3/GM}$ and the considered pulsation frequency, the pulsation frequencies ν_m of modes differing only by the m value of the spherical functions are linked through a simple relation. If we assume that the rotational frequency ν_{rot} is a function of the radius r only, this relation reads

$$\nu_m = \nu_0 + m \int_0^1 K(x)\nu_{\text{rot}}(x)\,dx, \qquad (1)$$

where $x = r/R$. The rotational kernel $K(x)$ depends on the considered mode (see Lynden-Bell & Ostriker 1967; Unno et al. 1989).

The $\ell = 1$, p_1 triplet and three components (corresponding to $m = -1, 1$ and 2) of the $\ell = 2$, g_1 quintuplet are observed. The components of these multiplets are not strictly equidistant as required by equation (1). These departures from equidistance may result from the fact that the rotation velocity of the star is too large for a linear approximation to be valid. It may also result from the fact that a magnetic field contributes to the splitting. As the departures from equidistance are not too large, we tentatively interpret them as errors in the measure of the splitting. So, we have $\Delta\nu_1 = 0.10\,375 \pm 0.005$ d^{-1} for mode $\ell = 1$, p_1 and $\Delta\nu_2 = 0.08\,457 \pm 0.003$ d^{-1} for mode $\ell = 2$, g_1, denoting by $\Delta\nu$ the integral term in equation (1).

Fig. 4 shows the behaviour of the rotational kernels for the modes we are investigating. It is clear that they do not probe the convective core. This was already the case for V836 Cen (Dupret et al. 2004) and, as in this case, with just two pieces of information on the behaviour of the rotation velocity, we analyse its trend inside the
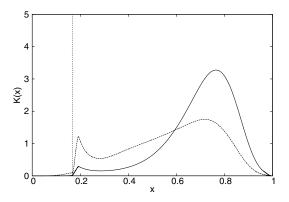

Figure 4. The kernels for the $\ell = 1$, p_1 mode (solid line) and for the $\ell = 2$, g_1 mode (dashed line). The vertical dotted line marks the position of the boundary of the convective core.

envelope by fitting the linear expression

$$\nu_{\text{rot}}(x) = \nu_{\text{rot},0} + \nu_{\text{rot},1}(x - 1). \qquad (2)$$

The splittings are then given by

$$\Delta\nu_k = c_{k0}\nu_{\text{rot},0} + c_{k1}\nu_{\text{rot},1} \quad k = 1, 2 \qquad (3)$$

with k referring to the two known splittings, and

$$c_{k0} = \int_0^1 K_k(x)\,dx, \qquad (4)$$

$$c_{k1} = \int_0^1 K_k(x)(x - 1)\,dx. \qquad (5)$$

Taking the errors on the splittings into account, the system (3) gives (all frequencies in d^{-1})

$$0.0878 < \nu_{\text{rot},0} < 0.1419\,, \quad -0.0491 < \nu_{\text{rot},1} < 0.0971\,.$$

The splitting data are thus consistent with a constant rotation velocity inside the envelope, a rotation period of 9.2 ± 2.2 d and an equatorial rotation velocity of 29 ± 7 km s^{-1}. This latter value is in full agreement with the $v \sin i$ and equatorial rotation velocity derived in Paper II.

6.2 Second-order analysis

A small asymmetry is observed in the $\ell = 1$ and $\ell = 2$ multiplets, as shown in Table 6. It is well known that asymmetries are explained by the effect of terms of higher order in $\nu_{\text{rot}}/\nu_{\text{puls}}$ in the pulsation equations. We determine here the adiabatic frequencies with the code FILOU (Tran Minh & Léon 1995; Suárez 2002). In the version of the code used here, the effects of rotation are included up to the second order, following Soufi et al. (1998). This code needs as input the spherically symmetric component of the structure model; it determines a posteriori the second-order deformation due to rotation. In principle, the gravity must be corrected for the effect of centrifugal acceleration already in the spherically symmetric component of the

Table 6. Observed rotational splittings (d^{-1}). The subscripts of $\nu_{\ell,m}$ denote the degree ℓ and azimuthal order m.

$\ell = 1$	$\nu_{1,0} - \nu_{1,-1}$	$\nu_{1,1} - \nu_{1,0}$	$\nu_{1,1} - \nu_{1,-1}$
	0.1083	0.0992	0.2075
$\ell = 2$	$(\nu_{2,1} - \nu_{2,-1})/2$	$\nu_{2,2} - \nu_{2,1}$	$\nu_{2,1} - \nu_{2,-1}$
	0.08\,605	0.0816	0.1721

Table 7. Theoretical rotational splittings (d^{-1}) obtained with a second-order perturbative treatment of rotation, for a model fitting the observed zonal modes.

Solid rotation: $\nu_{\mathrm{rot}} = 0.10\,751\,\mathrm{d}^{-1}$

$\ell = 1$	$\nu_{1,0} - \nu_{1,-1}$	$\nu_{1,1} - \nu_{1,0}$	$\nu_{1,1} - \nu_{1,-1}$
	0.10 934	0.09 816	0.2075
$\ell = 2$	$(\nu_{2,1} - \nu_{2,-1})/2$	$\nu_{2,2} - \nu_{2,1}$	$\nu_{2,1} - \nu_{2,-1}$
	0.08 661	0.08 859	0.1732

Solid rotation: $\nu_{\mathrm{rot}} = 0.10\,682\,\mathrm{d}^{-1}$

$\ell = 1$	$\nu_{1,0} - \nu_{1,-1}$	$\nu_{1,1} - \nu_{1,0}$	$\nu_{1,1} - \nu_{1,-1}$
	0.10 860	0.09 756	0.2062
$\ell = 2$	$(\nu_{2,1} - \nu_{2,-1})/2$	$\nu_{2,2} - \nu_{2,1}$	$\nu_{2,1} - \nu_{2,-1}$
	0.08 605	0.08 800	0.1721

Differential rotation: $\nu_{\mathrm{rot}} = 0.10\,915 + 0.00\,549(x-1)\,\mathrm{d}^{-1}$

$\ell = 1$	$\nu_{1,0} - \nu_{1,-1}$	$\nu_{1,1} - \nu_{1,0}$	$\nu_{1,1} - \nu_{1,-1}$
	0.10 932	0.09 819	0.2075
$\ell = 2$	$(\nu_{2,1} - \nu_{2,-1})/2$	$\nu_{2,2} - \nu_{2,1}$	$\nu_{2,1} - \nu_{2,-1}$
	0.08 605	0.08 826	0.1721

model. This correction would affect very slightly the frequencies (slow rotation) and has a negligible effect on the multiplet asymmetries. It is not included here, which allows us to use as input one of our best no-rotation model fitting the zonal mode frequencies, as determined in the previous sections. The main global parameters of this model are: $M = 8.4\,\mathrm{M}_{\odot}$, $\log(L/\mathrm{L}_{\odot}) = 3.7346$, $T_{\mathrm{eff}} = 22\,053\,\mathrm{K}$, $X = 0.72$, $Z = 0.014$ and $\alpha_{\mathrm{ov}} = 0.38$.

In Table 7, we give the theoretical rotational splittings obtained with this model and the second-order treatment of rotation. We recall that the second-order terms cancel in the combination $\nu_{\ell,m} - \nu_{\ell,-m}$. The last column gives such combination, which we use in the fitting procedure. Comparing Columns 1 and 2 shows the splitting asymmetry. For the first results given in this table, we consider a rigid rotation. In the first case, the rotation frequency is $\nu_{\mathrm{rot}} = 0.10\,751\,\mathrm{d}^{-1}$. With this value, we fit exactly the observed value of the $\ell = 1$ splitting: $\nu_{1,1} - \nu_{1,-1} = 0.2075\,\mathrm{d}^{-1}$. In the second case, the rotation frequency is $\nu_{\mathrm{rot}} = 0.10\,682\,\mathrm{d}^{-1}$. With this value, we fit exactly the observed value of the $\ell = 2$ splitting: $\nu_{2,1} - \nu_{2,-1} = 0.1721\,\mathrm{d}^{-1}$. In the last case of Table 7, we consider a differential rotation law of the same linear form as equation (2). The coefficients are adjusted to fit at the same time the observed $\ell = 1$ and $\ell = 2$ splittings $\nu_{1,1} - \nu_{1,-1}$ and $\nu_{2,1} - \nu_{2,-1}$. This gives the linear differential rotation law: $\nu_{\mathrm{rot}} = 0.10\,915 + 0.00\,549(x-1)\,\mathrm{d}^{-1}$. As for the first-order analysis, we see that rigid rotation models cannot be eliminated.

The results of Table 7 show that the non-equidistance of the $\ell = 1$ triplet is relatively well reproduced by the second-order effect of rotation. However, the asymmetries of the $\ell = 2$ multiplet do not fit the observations. This discrepancy could come from observations (multiplet not entirely resolved) or theory (effect of higher order terms). We did the same analysis with other models fitting the zonal mode frequencies and find quasi-identical results for the rotation velocity.

7 CONCLUSIONS

Our study of the β Cephei star θ Ophiuchi is a new illustration of the power of asteroseismology for this class of pulsators. The couple (X, Z) being chosen, the observation of three independent modes is enough to derive the other parameters that characterize a stellar model, for adopted physical inputs. We point out that such a success

can also be attributed to the unique derivation of (ℓ, m) thanks to the state-of-the-art empirical mode identification techniques used in Papers I and II.

A detailed NLTE abundance analysis showed that the considered abundance values, and thus the metallicity of θ Oph, corresponds to the new solar mixture of Asplund et al. (2005). In particular, the CNO abundances are much more consistent with the 3D values of Asplund et al. (2005) than with the 1D values of Grevesse & Sauval (1998). This is generally the case for B-type stars (Morel et al. 2006). We found a mass $M = 8.2 \pm 0.3\,\mathrm{M}_{\odot}$ and a central hydrogen abundance $X_{\mathrm{c}} = 0.38 \pm 0.02$ for the star. θ Oph is the fifth β Cephei star for which the occurrence of core overshooting is deduced by seismic interpretation and is the target with the highest derived value ($\alpha_{\mathrm{ov}} = 0.44 \pm 0.07$) among them. However, it might be that the core overshooting parameter of previously modelled β Cephei stars is underestimated, as the case of V836 Cen illustrates it. For the modelling of this star, Dupret et al. (2004) adopted a value of Z larger than 0.016 in order to get the excitation of the modes. However, Morel et al. (2006) determined $Z = 0.0105 \pm 0.0022$ for V836 Cen. In addition, Miglio et al. (2007) recently showed that modes can be excited for $Z \sim 0.01$ if one uses the new solar abundances together with the OP opacities, which was not the case in Dupret et al. (2004). Finally, considering a lower value of Z increases the α_{ov} of the star (see fig. 3 in Dupret et al. 2004).

We also showed that the asymmetry observed in the $\ell = 1$ triplet can be well reproduced by taking into account the effects of rotation up to the second order. For the quintuplet, the agreement is, however, not as good. Contrary to V836 Cen (Dupret et al. 2004) and ν Eri (Pamyatnykh et al. 2004) for which non-rigid rotation was proven, the observed rotational splitting of two modes for θ Oph is still compatible with a rigid rotation model. In the near future, we can expect stronger constraints on the internal rotation of β Cephei stars from data collected from space missions (e.g. MOST, COROT). With the observation of rotational splitting of many modes having different probing kernels, we aim to determine the internal rotation law of massive B-type stars.

REFERENCES

Aerts C., Marchenko S. V., Matthews J. M., 2006, ApJ, 642, 470
Aerts C., Thoul A., Daszyñska J., Scuflaire R., Waelkens C., Dupret M. A., Niemczura E., Noels A., 2003, Sci, 300, 1926
Aerts C. et al., 2004, A&A, 415, 241
Ausseloos M., Scuflaire R., Thoul A., Aerts C., 2004, MNRAS, 355, 352
Asplund M., Grevesse N., Sauval A. J., 2005, in Barnes T. G. III, Bash F. N., eds, ASP Conf. Ser. Vol. 336, Cosmic abundances as records of stellar evolution and nucleosynthesis. Astron. Soc. Pac., San Francisco, p. 25
Böhm-Vitense E., 1958, Z. Astrophys., 46, 108
Bourge P.-O., Alecian G., Thoul A., Scuflaire R., Théado S., 2006, Commun. Asteroseismol., 147, 105
Briquet M., Lefever K., Uytterhoeven K., Aerts C., 2005, MNRAS, 362, 619 (Paper II)
Caughlan G. R., Fowler W. A., 1988, At. Data Nucl. Data Tables, 40, 283
Cunha K., Hubeny I., Lanz T., 2006, ApJ, 647, L143

Daflon S., Cunha K., 2004, ApJ, 617, 1115

De Ridder J. et al., 2004, MNRAS, 351, 324

Deupree R. G., 2000, ApJ 543, 395

Dupret M.-A., 2001, A&A, 366, 166

Dupret M.-A., Thoul A., Scuflaire R., Daszyñska-Daszkiewicz J., Aerts C., Bourge P.-O., Waelkens C., Noels A., 2004, A&A, 415, 251

Ferguson J. W., Alexander D. R., Allard F., Barman T., Bodnarik J. G., Hauschildt P. H., Heffner-Wong A., Tamanai A., 2005, ApJ, 623, 585

Formicola A. et al., 2004, Phys. Lett. B, 591, 61

Grevesse N., Sauval A. J., 1998, Space Sci. Rev., 85, 161

Handler G., Shobbrook R. R., Mokgwetsi T., 2005, MNRAS, 362, 612 (Paper I)

Kaiser A., 2006, in Sternken C., Aerts C., eds, ASP Conf. Ser. Vol. 349 Astrophysics of Variable Stars. Astron. Soc. Pac., San Francisco, p. 257

Kurucz R. L., 1993, ATLAS9 Stellar Atmosphere Programs and 2 km s^{-1} grid. Kurucz CD-ROM No. 13. Smithsonian Astrophysical Observatory, Cambridge, Massachusetts, p. 13

Lynden-Bell D., Ostriker J. P., 1967, MNRAS, 136, 293

Mazumdar A., Briquet M., Desmet M., Aerts C., 2006, A&A, 459, 589

McAlister H., Mason B. D., Hartkopf W. I., Shara M. M., 1993, AJ, 106, 1639

Miglio A., Montalbán J., Dupret M.-A., 2007, MNRAS, 375, 21

Morel T., Butler K., Aerts C., Neiner C., Briquet M., 2006, A&A, 457, 651

Niemczura E., Daszynska-Daszkiewicz J., 2005, A&A, 433, 659

Pamyatnykh A. A., Handler G., Dziembowski W. A., 2004, MNRAS, 350, 1022

Puls J., Urbaneja M. A., Venero R., Repolust T., Springmann U., Jokuthy A., Mokiem M. R., 2005, A&A, 435, 669

Ribas I., Jordi C., Gimenez A., 2000, MNRAS, 318, 55

Rogers F. J., Nayfonov A., 2002, ApJ, 576, 1064

Scuflaire R., Théado S., Montalban J., Miglio A., Bourge P.-O., Godart M., Thoul A., Noels A., 2007a, Ap&SS, 322, in press

Scuflaire R., Montalban J., Théado S., Bourge P.-O., Miglio A., Godart M., Thoul A., Noels A., 2007b, Ap&SS, 322, in press

Seaton M. J., 2005, MNRAS, 362, L1

Smalley B., Dworetsky M. M., 1995, A&A, 293, 446

Soufi F., Goupil M.-J., Dziembowski W. A., 1998, A&A, 334, 911

Suárez J. C., 2002, PhD thesis, Observatoire de Paris

Talon S., Zahn J.-P., Maeder A., Meynet G., 1997, A&A, 322, 209

Thoul A., Bahcall J., Loeb A., 1994, ApJ, 421, 828

Tran Minh F., Léon L., 1995, Phys. Process Astrophys., 458, 219

Unno W., Osaki Y., Ando H., Saio H., Shibahashi H., 1989, Nonradial Oscillations of Stars. University of Tokyo Press, Tokyo

This paper has been typeset from a T$_{\rm E}$X/L$^{\rm A}$T$_{\rm E}$X file prepared by the author.